ESTIMATION OF THE THREE-DIMENSIONAL SPACE SPEED OF A CORONAL MASS EJECTION USING METRIC RADIO DATA

C. KATHIRAVAN

Indian Institute of Astrophysics, Bangalore 560 034, India; kathir@iiap.res.in

AND

R. RAMESH

Centre for Research and Education in Science and Technology, Indian Institute of Astrophysics, Hosakote 562 114, India; ramesh@iiap.res.in

Received 2003 December 16; accepted 2004 March 25

ABSTRACT

We present an independent method for obtaining the three-dimensional space speed of a coronal mass ejection in the lower solar atmosphere through ray-tracing analysis of the thermal radio counterpart of its frontal loop in the metric wavelength range. The scheme was tested on the halo event observed on 1998 January 21, obtaining an estimated space speed of 580 km s^{-1}. We also separately calculated the speed along the line of sight and in the plane of the sky, obtaining values of $\approx$318 and 485 km s^{-1}, respectively.

Subject headings: solar-terrestrial relations — Sun: activity — Sun: corona — Sun: radio radiation

1. INTRODUCTION

Studies of the influence of solar activity on our terrestrial environment have taken on increasing importance in recent years in response to the realization of just how damaging space influences can be. It is well accepted now that the state of the near-Earth space environment is significantly controlled by coronal mass ejections (CMEs), the most geoeffective manifestation of solar activity (Gosling et al. 1991). The observations made with conventional "white light" coronagraphs are the historical and empirical foundations of our present knowledge of CMEs. However, by their very nature the coronagraphs have an occulting disk to block the direct photospheric light and so the early life/kinematics of a CME in the low corona cannot be studied using them. This is very important, particularly in the case of halo CMEs (Howard et al. 1982) that originate from the front side of the Sun, since they are more likely to reach Earth's environment. What one usually measures from a time-lapse movie of the images obtained with a coronagraph is the speed at which a CME spreads in the plane of the sky. This will at best be only a lower limit to the true speed (space speed), especially in the case of Earth-directed halo CMEs, since they lie away from the plane of the sky. Attempting to obtain the true speed of a CME whose source region lies on the solar disk is a widely pursued area of research in CME studies (Fisher & Munro 1984; Eselevich & Filippov 1991; Hundhausen et al. 1994; Plunkett et al. 1998; Sheeley et al. 1999; Leblanc et al. 2001; Zhao et al. 2002; Michalek et al. 2003; Reiner et al. 2003). Ray-tracing analysis of the thermal radio counterpart of a CME in the metric wavelength range plays a vital role in this connection, since one can localize the position of the associated density enhancement in a three-dimensional space (Kathiravan et al. 2002). Also, it is to be noted that radio observations do not have the limitation of an occulting disk and CMEs can be detected early in their development. One can observe activity at any longitude similar to that at EUV and X-ray wavelengths (Ramesh 2000). In addition, the frontal structure of a CME has a large optical depth at meter wavelengths and can be readily observed (Bastian & Gary 1997; Gopalswamy 1999; Ramesh et al. 2003). Making use of the above-mentioned advantages, we present an independent method for estimating the three-dimensional space speed of a CME close to its onset using metric radio data.

2. THE METHOD

The brightness distribution of the "quiet" Sun was computed theoretically from centimeter to meter wavelengths for the first time by Smerd (1950). He assumed a spherically symmetric corona to derive the solution by numerical integration of the radiative transfer equation for an ionized medium. The existence of density enhancements make the corona asymmetric, and one has to resort to a more involved ray-tracing technique to derive the brightness distribution. Such calculations were carried out by Newkirk (1961); he derived the brightness profiles at short wavelengths. Sastry et al. (1983) used a ray-tracing technique similar to that of Newkirk to explain the one-dimensional brightness distribution observed by them in the decameter wavelength range. Recently, we successfully extended the above scheme to the analysis of an observed two-dimensional thermal radio brightness distribution (Kathiravan et al. 2002). One of the interesting results that came out of our calculations was the possibility of obtaining the location of the various discrete sources along the line-of-sight direction also, in a straightforward manner. This provides us with a technique to determine the three-dimensional position coordinates of the thermal radio counterpart of a density enhancement in the corona at a given epoch and estimate its space speed under situations where it shows noticeable displacement as a function of time.

The brightness temperature (T_b) for any ray path is given by

$$T_b(a) = \int_{\tau_1}^{\tau_2} T_e[1 - e^{-\tau(a)}]\,d\tau, \tag{1}$$

where T_e is the electron kinetic temperature of the corona, τ is the optical depth along the ray path, and a is the distance between the Sun-Earth line and the ray trajectory at the point where they are parallel. Starting at a distance of 5 $R_\odot$ away from the front side of the Sun, each ray is first traced through the solar atmosphere (in the direction of the Sun) up to the

plasma layer, where it gets reflected/refracted, and then continued for a similar distance (away from the Sun) in either the backward or a different direction depending on the case. Here τ is estimated using the expression

$$\tau = \int_{s_1}^{s_2} k(s)\,ds, \tag{2}$$

where $k = \left(0.16N_e^2\right)/\left(f^2\mu T_e^{1.5}\right)$ is the absorption coefficient and s is the path length along the ray. Here s_1 and s_2 are the limits for the infinitesimal path length (ds) chosen; μ and f are the refractive index and frequency chosen for ray tracing, respectively. Although in principle one could use any standard electron density distribution model for the solar corona in which the rays are to be traced, we describe our technique using the model of Newkirk (1961). The electron density at any point in the corona is given by

$$N_e(\rho) = N_0\left[1 + C_n \exp\left(-\beta^2\right)\right] \text{ cm}^{-3}, \tag{3}$$

where $N_0 = 4.2 \times 10^{4.32/\rho}$ (the spherically symmetric component of the background "quiet" Sun), the constant C_n is the strength of the density enhancement/depletion, and β depends on its location and size. It is given by

$$\beta^2 = \frac{(x - x_0)^2}{2\sigma_x^2} + \frac{(y - y_0)^2}{2\sigma_y^2} + \frac{(z - z_0)^2}{2\sigma_z^2} \tag{4}$$

where σ_x, σ_y, σ_z, and x_0, y_0, z_0 are the size (along the respective axes) and the location of the centroid of the density enhancement/depletion, respectively. Here x is toward the Earth, i.e., along the line of sight, and y and z represent the longitudinal and latitudinal directions on the Sun, respectively. All distances are in units of $R_\odot$ ($R_\odot = 1$ solar radius = 6.96×10^5 km). For the localized regions, we use a model in which the density falls off as a Gaussian function along the x, y, and z directions from their centroid. Equation (1) is evaluated for different values of y and z to get a two-dimensional map of the brightness distribution. In practice, the above step may have to be repeated several times using various values for the position and strength of the density enhancement to get a good fit for a particular observed distribution. It is obvious that if the observed distribution evolves with time, then the different parameters used in the ray-tracing calculations will be unique to the radio map obtained at a particular epoch. It is this feature of the scheme that we are trying to make use of in estimating the true speed of a CME through ray-tracing analysis of its thermal radio counterpart imaged at different time intervals in the metric wavelength range.

3. APPLICATION TO THE HALO CME OF 1988 JANUARY 21

3.1. *Observations*

The radio data reported were obtained on 1998 January 21 with the Gauribidanur radioheliograph (GRH; see Ramesh et al. 1998 for details on the instrument), operating near Bangalore in India. The observing frequency was 109 MHz. The minimum detectable flux limit of the array is ∼0.02 SFU (1 SFU = 10^{-22} W m^{-2} Hz^{-1}) and the angular resolution is ∼$7' \times 11'$ (R.A. × decl.) at the above frequency. The field of

view is ∼$3° \times 5°$. The calibration scheme used for processing the data obtained with GRH makes use of the available redundancy in the length and orientation of the various baseline vectors and allows us to image sources with a dynamic range of >20 dB (Ramesh 1998; Ramesh et al. 1999). This allows us to detect faint thermal features associated with density enhancements such as streamers, CMEs, etc., in the solar atmosphere. According to the CME catalog for the year 1998, a full halo event was observed on 1998 January 21 by the Large Angle and Spectrometric Coronagraph (LASCO; Brueckner et al. 1995) on board the *Solar and Heliospheric Observatory* (*SOHO*; Fleck et al. 1995). The event was first observed above the southern quadrant of the occulting disk of the LASCO C2 coronagraph around 06:37:25 UT. Its leading edge was located at a height of ∼2.75 $R_\odot$ at that time. The estimated linear speed of the leading edge of the CME in the plane of the sky was 361 km s^{-1}. The extrapolated onset time of the event from the center of the Sun was 05:09:09 UT.[1] Figure 1 shows a difference image of the event obtained at 07:32 UT by subtracting a pre-event image taken at 06:06 UT. One can notice the CME as a faint ringlike feature in the southern hemisphere. The event was associated with a Hα filament disappearance from location S57, E19 on the solar disk between 04:00 and 06:03 UT on that day (Gopalswamy et al. 2000; Zhou et al. 2003; Solar-Geophysical Data, 647, Part II, 1998 July). Figures 2 and 3 show the radioheliogram obtained with GRH on 1998 January 21 around 05:01:06 and 06:01:06 UT, respectively. Figure 4 shows the difference of the above two images, i.e., 06:01:06−05:01:06 UT. Note the enhanced radio emission at approximately the same location as the leading edge of the white light CME in the LASCO C2 difference image in Figure 1. The radio Sun was very "quiet" and no nonthermal activity was reported, particularly during our observing period (Solar-Geophysical Data, 643, Part I, 1998 March). This indicates that the emission seen in Figure 4 is most likely due to thermal bremmstrahlung from the excess electrons (above the ambient) in the frontal loop of the white light CME and is the radio counterpart of the latter.

3.2. *Analysis and Results*

Figure 5 shows the brightness distribution obtained using the ray-tracing technique described above for the observed radio map in Figure 3. There is a striking similarity between them. We assumed a background corona of uniform brightness temperature ($T_e = 1.0 \times 10^6$ K) and a density profile equal to 0.5 times that given by Newkirk's model for the calculations. The parameters of the various localized sources used are listed in Table 1. A comparison of Figure 5 with the difference map in Figure 4 shows that there is a good correspondence between the location of the excess emission in the southern hemisphere of the latter and the sources s8, s9, . . ., and s13 in the former. This suggests that the above set of discrete sources comprise the radio CME. Its total mass (M_{radio}) is given by

$$M_{\text{radio}} = m_8 + m_9 + m_{10} + m_{11} + m_{12} + m_{13}, \tag{5}$$

where m_8, m_9, . . ., and m_{13} represent the mass of the structures s8, s9, . . ., s13, respectively. These masses were calculated by multiplying the volume of each structure with the electron density at the location of their corresponding

---

[1] The *SOHO*/LASCO CME catalog is at http://cdaw.gsfc.nasa.gov/ CME_list.
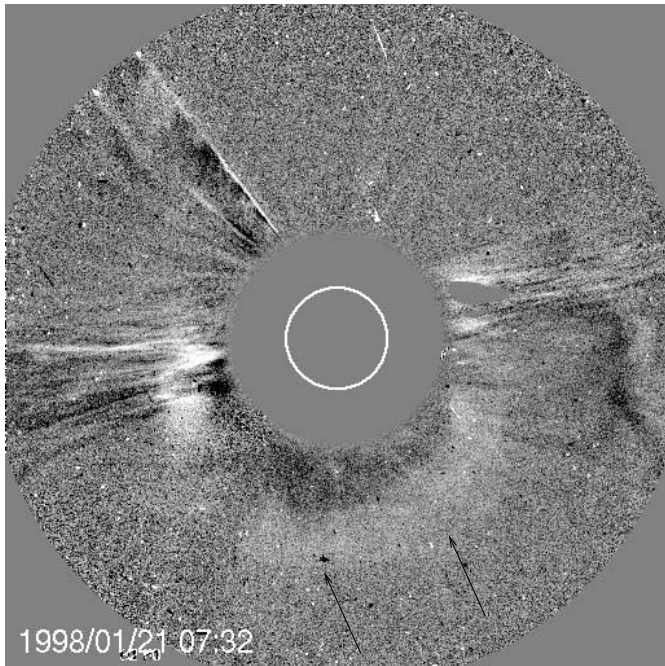
FIG. 1.—Difference image (07:32−06:06 UT) of the halo CME event observed with the LASCO C2 coronagraph on 1998 January 21. The inner open circle indicates the solar limb. The outer filled circle is the occulting disk of the coronagraph. It extends approximately up to 2.2 $R_\odot$ from the center of the Sun. Solar north is straight up and east is to the left. The CME under study can be seen as a faint ring (indicated by the arrow marks) above the occulter of the coronagraph in the southern quadrant.
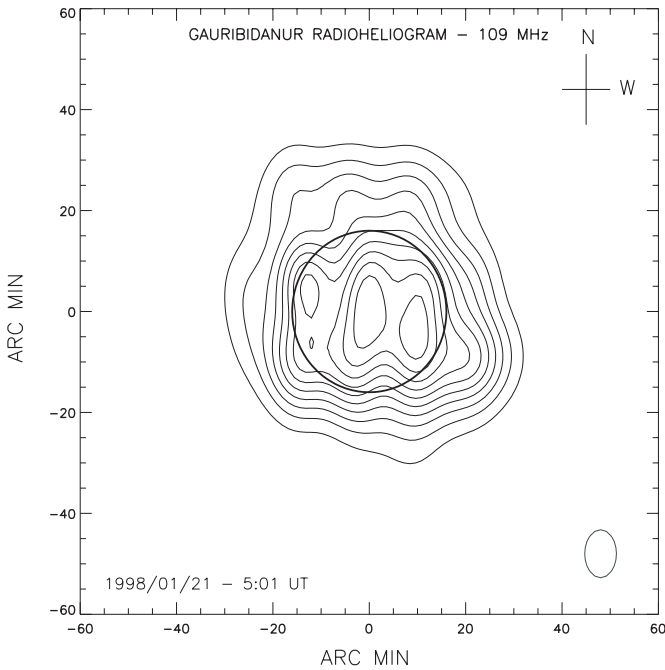

FIG. 3.—Same as Fig. 2, but obtained at 06:01 UT. The peak brightness temperature is ∼1×10^6 K and the contour interval is 1×10^5 K.

FIG. 2.—Radioheliogram obtained with GRH at 109 MHz on 1998 January 21 at 05:01 UT. The peak brightness temperature is ∼1.21×10^6 K and the contour interval is 1×10^5 K. The open circle at the center is the solar limb. The instrument beam is shown near the bottom-right corner.
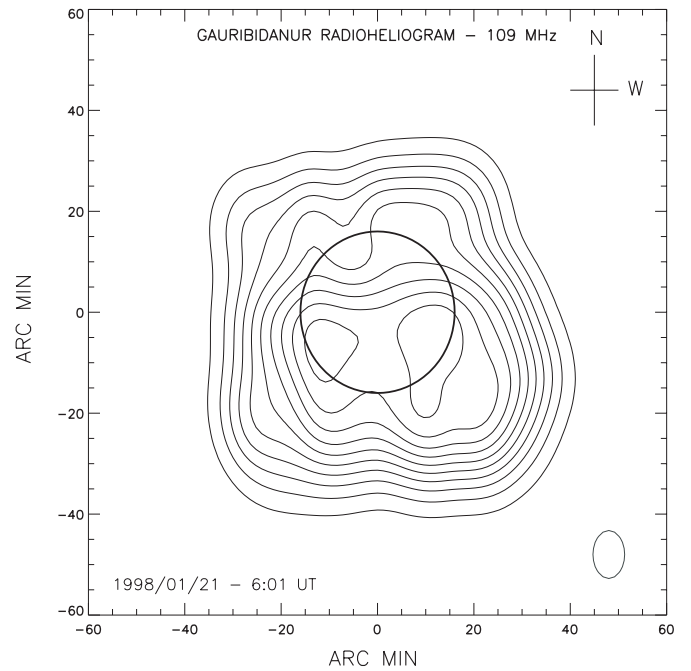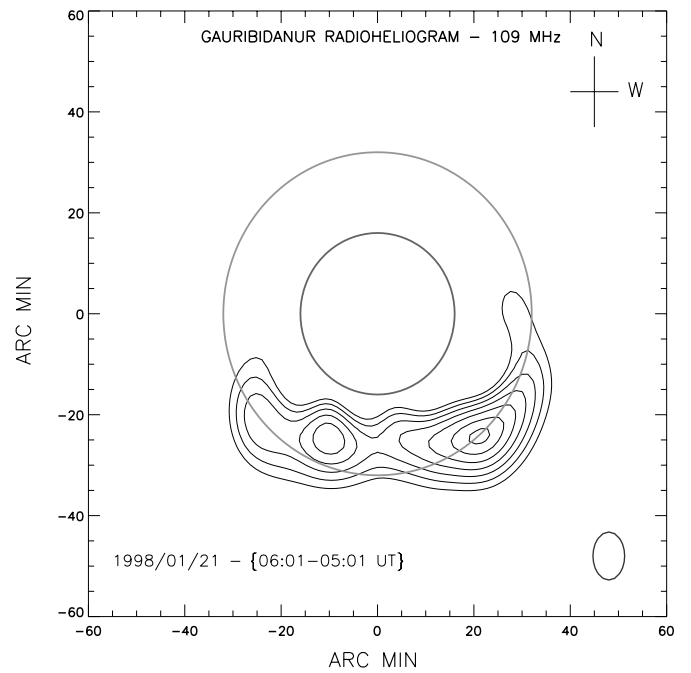

FIG. 4.—Difference map obtained by subtracting the radioheliogram in Fig. 2 (05:01 UT) from that in Fig. 3 (06:01 UT). Only contours with levels greater than 50% of the peak value are shown here. The enhanced radio emission in the southern hemisphere correlates well with the leading edge of the white light CME in Fig. 1. The outer larger circle in the map corresponds approximately to the occulter size of the LASCO C2 coronagraph.
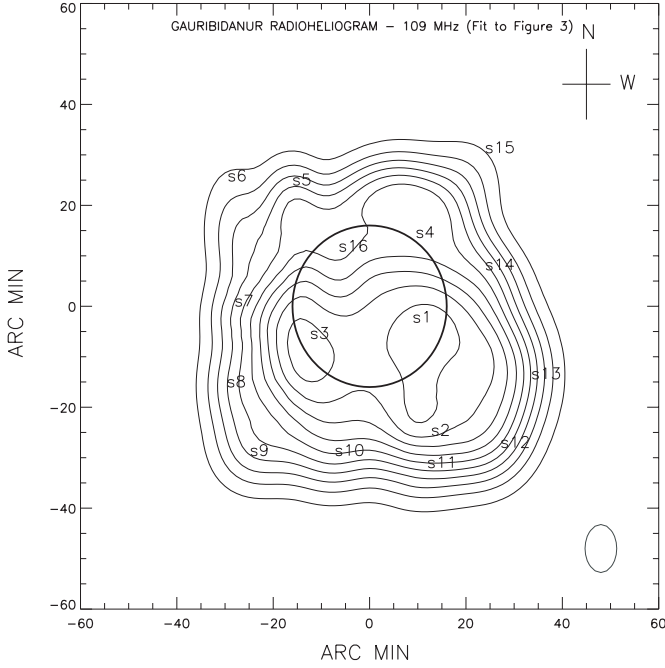
FIG. 5.—Radio brightness distribution of the Sun obtained through ray-tracing calculations of the GRH data obtained at 06:01 UT (Fig. 3). There is a good correspondence between the two distributions. The numbers s1–s16 indicate the location of the centroid of the discrete sources listed in Table 1.

of 1998 January 21 was closely associated with the disappearance of the Hα filament from the location S57°, E19° on the solar disk. Assuming this location to be on the solar surface, i.e., at a radial distance of 1 $R_\odot$ (in three-dimensional space) from the center of the Sun, we calculated its position vector to be $\boldsymbol{R}_{\mathrm{H}\alpha} = 0.51\hat{x} - 0.18\hat{y} - 0.84\hat{z}$. According to the LASCO CME catalog, the lift-off time of the aforementioned halo CME projected to 1 $R_\odot$ is 05:41:17 UT. The above time was obtained by employing a linear fit to the LASCO C2/C3 height-time measurements of the leading edge of the white light CME in the plane of the sky, and is for the case where the CME is considered to travel at a constant speed. Note that in the present case, we have assumed that the source region of the CME on the solar disk is S57°, E19°, i.e., the location of the Hα filament. This corresponds to a radial distance of ≈0.86 $R_\odot$ in the plane of the sky. We estimated the lift-off time of the CME from the above location by back projecting its height-time curve; this lift-off time is 05:37:26 UT. This implies that the CME had traveled a distance of ~824,253 km (i.e., $[(\boldsymbol{R}_{\mathrm{radio}} - \boldsymbol{R}_{\mathrm{H}\alpha})^2]^{1/2}$) in the three-dimensional space during the time interval 06:01:06–05:37:26 UT, i.e., at an average speed of ≈580 km s^{-1}. Note that this value should be treated with caution, since we have assumed that the CME was propagating at a constant speed. Unfortunately, we do not have more radio data to calculate the speed of the CME independent of its onset time from the solar surface and without any assumption.

centroid. If $\boldsymbol{R}_{\mathrm{radio}}$ indicates the position vector of the radio CME, then we have

$$\boldsymbol{R}_{\mathrm{radio}} = \frac{1}{M_{\mathrm{radio}}}(m_8\boldsymbol{r}_8 + m_9\boldsymbol{r}_9 + m_{10}\boldsymbol{r}_{10} + m_{11}\boldsymbol{r}_{11} + m_{12}\boldsymbol{r}_{12} + m_{13}\boldsymbol{r}_{13}). \quad (6)$$

Here $\boldsymbol{r}_8, \boldsymbol{r}_9, \ldots, \boldsymbol{r}_{13}$ represent the position vector of the radio structures s8, s9, . . . , s13, respectively. Substituting for the different values in equations (5) and (6), we get $\boldsymbol{R}_{\mathrm{radio}} = 1.16\hat{x} + 0.52\hat{y} - 1.54\hat{z}$. As pointed out earlier, the halo CME

4. CONCLUSIONS

We have presented an independent technique for the estimation of the three-dimensional space speed of a CME near the Sun through ray-tracing analysis of the enhanced thermal radio emission from its frontal loop in the metric wavelength regime. We successfully applied the method to obtain the space speed of the halo CME observed on 1998 January 21 with GRH at 109 MHz, obtaining a value of ≈580 km s^{-1}. We also separately calculated its speed along the line of sight and in the plane of the sky, these being ≈318 and 485 km s^{-1}, respectively. Michalek et al. (2003) had obtained the "corrected" speed for the same event using the data obtained with

TABLE 1
PARAMETERS OF THE DISCRETE SOURCES USED IN THE RAY-TRACING CALCULATIONS

Source	Centroid[a] ($R_\odot$)	Size[b] ($R_\odot$)	Density Factor[c]	Temperature Factor[c]
s1	1.72, 0.56, −0.20	0.32, 0.74, 0.59	34.0	1.20
s2	1.60, 0.80, −1.60	0.32, 0.47, 0.52	16.0	0.58
s3	1.70, −0.77, −0.40	0.22, 0.55, 0.71	18.0	0.92
s4	1.10, 0.60, 0.85	0.22, 0.63, 0.77	18.0	0.63
s5	1.00, −1.00, 1.50	0.22, 0.22, 0.50	8.0	0.20
s6	0.60, −1.84, 1.55	0.22, 0.32, 0.77	7.0	0.20
s7	1.10, −1.75, 0.00	0.22, 0.32, 0.32	7.5	0.20
s8	0.80, −1.85, −1.00	0.22, 0.32, 0.45	9.0	0.20
s9	1.20, −1.55, −1.85	0.22, 0.45, 0.45	17.3	0.20
s10	1.30, −0.45, −1.85	0.22, 0.39, 0.52	12.4	0.20
s11	1.00, 0.75, −2.00	0.22, 0.45, 0.50	10.0	0.20
s12	1.00, 1.70, −1.75	0.22, 0.45, 0.50	22.0	0.40
s13	1.40, 2.10, −0.90	0.22, 0.45, 0.67	22.0	0.60
s14	1.10, 1.50, 0.45	0.22, 0.45, 0.32	10.0	0.20
s15	0.40, 1.50, 1.90	0.22, 0.19, 0.39	7.0	0.20
s16	1.70, −0.40, 0.68	0.22, 0.19, 0.39	−0.3	−0.30

[a] In x, y, and z coordinates.
[b] Along x, y, and z axes.
[c] Positive and negative values correspond to enhancement and decrement, respectively.

the LASCO C2 and C3 coronagraphs, obtaining a value of ≈ 468 km s^{-1}, i.e., somewhat (but not much) lower than our estimate. Nevertheless, this example vividly illustrates the role of radio-imaging observations in the estimation of the inner coronal kinematics of CMEs. The only prerequisites of the method are (1) that the CME should not be accompanied by any intense nonthermal emission (particularly the long-lasting type I noise-storm continuum) as in the present case, and (2) that it should occur during the observing period of the particular instrument. This is a serious drawback that limits the usefulness of the scheme at present. The first limitation can be overcome to a large extent through well-defined calibration procedures. We are in the process of installing a full-fledged tracking system for GRH that will enable us to carry out continuous observations of the Sun for ~6 hr ($\approx$03:30–09:30 UT) every day. In the future, we intend to estimate the space speed and acceleration of CMEs that occur (during the above period) in the low corona solely using radio data obtained with GRH. Using the *SOHO*/LASCO CME catalog, Gopalswamy et al. (2004) recently showed that the rate of occurrence of CMEs is ~0.5 and 6 day^{-1} during solar minimum and maximum, respectively. Given the limited duration of our observations and the capabilities of the instrument, we therefore expect to study the characteristics of the initial evolution of 1 or 2 CMEs every day, particularly during the solar maximum period. During the solar minimum period, we would be fortunate to have the onset of the CME during our observing period. But with advanced radio-imaging instruments like the Frequency Agile Solar Radiotelescope (FASR) and Low Frequency Array (LOFAR) to become available, the number might increase significantly in the coming years.

REFERENCES

Bastian, T. S., & Gary, D. E. 1997, J. Geophys. Res., 102, 14031
Brueckner, G. E., et al. 1995, Sol. Phys., 162, 357
Eselevich, V. G., & Filippov, M. A. 1991, Planet. Space Sci., 39, 737
Fisher, R. R., & Munro, R. H. 1984, ApJ, 280, 428
Fleck, B., Domingo, V., & Poland, A. I. 1995, The *SOHO* Mission (Dordrecht: Kluwer)
Gopalswamy, N. 1999, in Proc. Nobeyama Symp., Solar Physics with Radio Observations, ed. T. Bastian, N. Gopalswamy, & K. Shibasaki (NRO Rep. 479; Kiyosato: Nobeyama Radio Obs.), 141
Gopalswamy, N., Lara, A., Yashiro, S., Nunes, S., & Howard, R. A. 2003, in Proc. ISCS Symp., Solar Variability as an Input to the Earth's Environment, ed. A. Wilson (ESA SP-535; Noordwijk: ESA), 403
Gopalswamy, N., et al. 2000, Geophys. Res. Lett., 27, 1427
Gosling, J. T., McComas, D. J., Phillips, J. L., & Bame, S. J. 1991, J. Geophys. Res., 96, 7831
Howard, R. A., Michels, D. J., Sheeley, N. R., Jr., & Koomen, M. J. 1982, ApJ, 263, L101
Hundhausen, A. J., Burkepile, J. T., & St. Cyr, O. C. 1994, J. Geophys. Res., 99, 6543
Kathiravan, C., Ramesh, R., & Subramanian, K. R. 2002, ApJ, 567, L93
Leblanc, Y., Dulk, G. A., Vourlidas, A., & Bougeret, J.-L. 2001, J. Geophys. Res., 106, 25301

Michalek, G., Gopalswamy, N., & Yashiro, S. 2003, ApJ, 584, 472
Newkirk, G., Jr. 1961, ApJ, 133, 983
Plunkett, S. P., Thompson, B. J., Howard, R. A., Michels, D. J., St. Cyr, O. C., Tappin, S. J., Schwenn, R., & Lamy, P. L. 1998, Geophys. Res. Lett., 25, 2477
Ramesh, R. 1998, Ph.D. thesis, Bangalore Univ.
———. 2000, Sol. Phys., 196, 213
Ramesh, R., Kathiravan, C., & Sastry, C. V. 2003, ApJ, 591, L163
Ramesh, R., Subramanian, K. R., & Sastry, C. V. 1999, A&AS, 139, 179
Ramesh, R., Subramanian, K. R., Sundararajan, M. S., & Sastry, C. V. 1998, Sol. Phys., 181, 439
Reiner, M. J., Vourlidas, A., St. Cyr, O. C., Burkepile, J. T., Howard, R. A., Kaiser, M. L., Prestage, N. P., & Bougeret, J.-L. 2003, ApJ, 590, 533
Sastry, C. V., Shevgaonkar, R. K., & Ramanuja, M. N. 1983, Sol. Phys., 87, 391
Sheeley, N. R., Jr., Walters, J. H., Wang, Y.-M., & Howard, R. A. 1999, J. Geophys. Res., 104, 24739
Smerd, S. F. 1950, Australian J. Sci. Res., A3, 34
Zhao, X. P., Plunkett, S. P., & Liu, W. 2002, J. Geophys. Res., 107, 1223
Zhou, G., Wang, J., & Cao, Z. 2003, A&A, 397, 1057